Nitro-Pyrazinotriazapentalene scaffolds– nitroreductase quantification and in vitro fluorescence imaging of hypoxia

Ewelina Janczy-Cempa, Olga Mazuryk, Doina Sirbu, Nicolas Chopin, Magdalena Żarnik, Magdalena Zastawna, Cyril Colas, Marie-Aude Hiebel, Franck Suzenet, Malgorzata Brindell

Sensors & Actuators: B. Chemical 346 (2021) 130504

Contents lists available at ScienceDirect

Sensors and Actuators: B. Chemical

journal homepage: www.elsevier.com/locate/snb

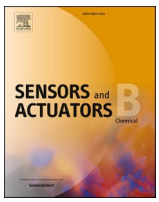

Nitro-Pyrazinotriazapentalene scaffolds– nitroreductase quantification and *in vitro* fluorescence imaging of hypoxia

Ewelina Janczy-Cempa [a], Olga Mazuryk [a], Doina Sirbu [b], Nicolas Chopin [b], Magdalena Żarnik [a,b], Magdalena Zastawna [a,b], Cyril Colas [b,c], Marie-Aude Hiebel [b], Franck Suzenet [b,*], Małgorzata Brindell [a,*]

[a] Department of Inorganic Chemistry, Faculty of Chemistry, Jagiellonian University in Kraków, Gronostajowa 2, 30-387, Krakow, Poland
[b] Institute of Organic and Analytical Chemistry, University of Orléans, UMR-CNRS 7311, rue de Chartres, BP 6759, 45067, Orléans Cedex 2, France
[c] Center for Molecular Biophysics, CNRS UPR 4301, University of Orléans, rue Charles Sadron, 45071, Orléans Cedex 2, France

ARTICLE INFO

Keywords:
Fluorescent probe
Nitroreductase
Hypoxia
Imaging
Albumin

ABSTRACT

Nitroreductases (NTRs), a family of flavin-containing enzymes, can be overexpressed in regions of tumor hypoxia, *i.e.*, areas deprived of oxygen. The detection of NTR may be applied for monitoring the hypoxia level in tumors. To quantify NTR, novel sensors were designed based on the conjugation of pyridazino-1,3a,6a-triazapentalene to a *para*-nitrophenyl, directly or with an alkyne linker, resulting in two probes denoted as **1-NO_2** and **2-NO_2**. Both probes had a weak fluorescence (form *off*), while their reduction by NTR led to the over 15-fold enhancement of fluorescence intensity (form *on*) regardless of the oxygen concentration in their environment. The detection limit was as low as ca. 20−30 ng/mL of NTR. Interestingly, the presence of human serum albumin significantly enhanced the observed fluorescence turned on by NTR in particular for the **2-NO_2** probe. The *in vitro* response to both probes was evaluated on the highly metastatic human melanoma A2058 cell line, where NTR levels increased under hypoxic conditions. Their low toxicity, high photostability, and efficient uptake combined with a strong correlation between the enhancement of fluorescence and hypoxia in cells indicate the high potential of the **1-NO_2** and **2-NO_2** probes for the assessment of the hypoxic environment in biomedical research. The designed compounds allowed for a fast determination of the difference in NTR content of cells without the need for special sample preparation such as cell lysis. The changes can be monitored using a plate reader, flow cytometer, and fluorescence microscope, which that makes these probes a remarkably universal tool.

1. Introduction

Nitroreductases (NTRs) are a family of flavin-containing enzymes, which can reduce the nitroaromatic compounds using reduced NAD(P)H as an electron donor. NTRs take part in detoxification [1] however, the major interest in NTRs is related to using them to activate bioreductive prodrugs [2,3] or to evaluate the regions with low oxygen levels in tumors, which are generally termed as hypoxia [4]. The existence of hypoxia within tumors and subsequent information about its relation and contribution to poor prognosis and treatment failure [5] provided a rationale for the development of tools helping in the evaluation of the hypoxia level. It was presumed that in cancer cells, hypoxia can promote overexpression of the reductive enzymes, such as NTRs, azoreductase, quinone reductase, cytochrome P450 reductase, xanthine oxidase, and others [6–8]. Despite the utilization of this feature for many years the relationship between the expression of these enzymes and the degree of hypoxia is largely unknown. To the best of our knowledge, the literature does not provide data on the direct quantification of selected enzymes in cells grown under normoxic *vs* hypoxic conditions. In this study, we demonstrate for the first time with a pyrazinotriazapentalene based probe that indeed there is an elevated level of NTR in highly metastatic human melanoma cells, line A2058, cultured under hypoxic conditions. This finding justifies our research focusing on new probes, that assess nitroreductase activity as potential markers for detection of hypoxia.

Two types of NTRs are known. Type I, which is oxygen-insensitive and can catalyze reduction in the presence of molecular oxygen, and type II, which is oxygen-sensitive and only functions well under extreme hypoxia conditions [9,10]. Type I of NTRs conducts two-electron

* Corresponding authors.
E-mail addresses: franck.suzenet@univ-orleans.fr (F. Suzenet), malgorzata.brindell@uj.edu.pl (M. Brindell).

https://doi.org/10.1016/j.snb.2021.130504
Received 26 May 2021; Received in revised form 13 July 2021; Accepted 24 July 2021
Available online 27 July 2021

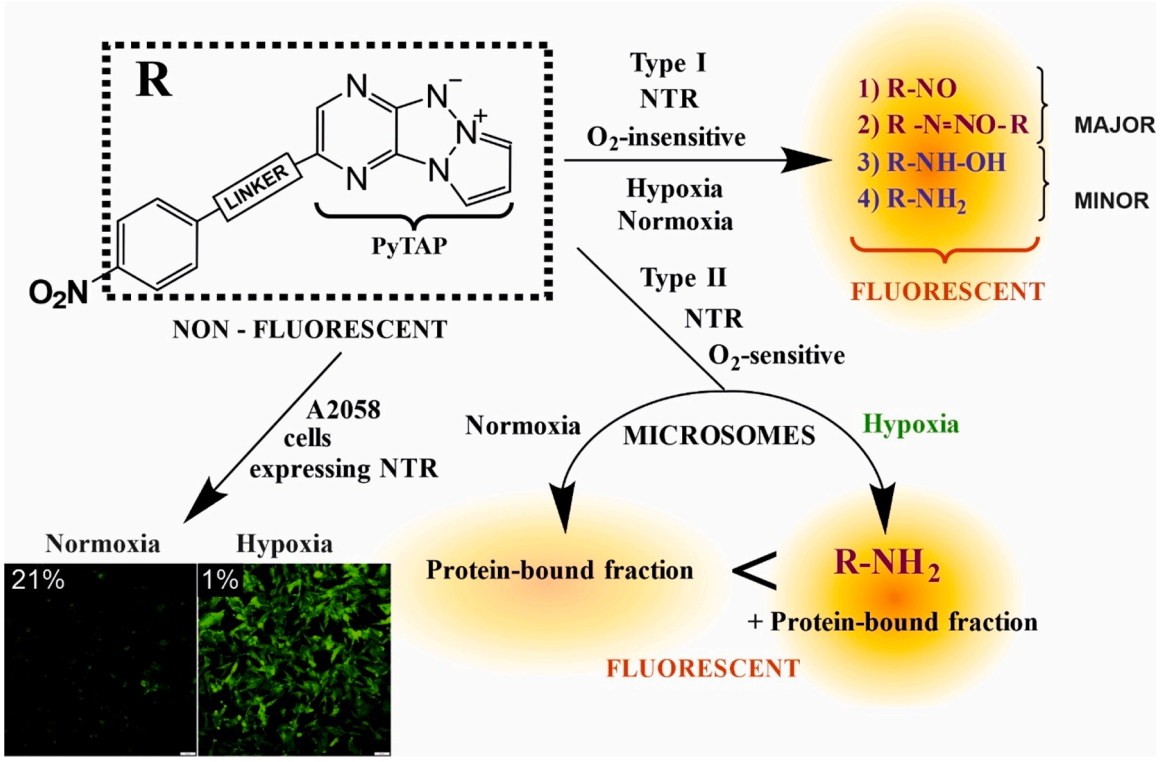

Chart 1. Schematic representation of the major outcomes of the investigated probes.

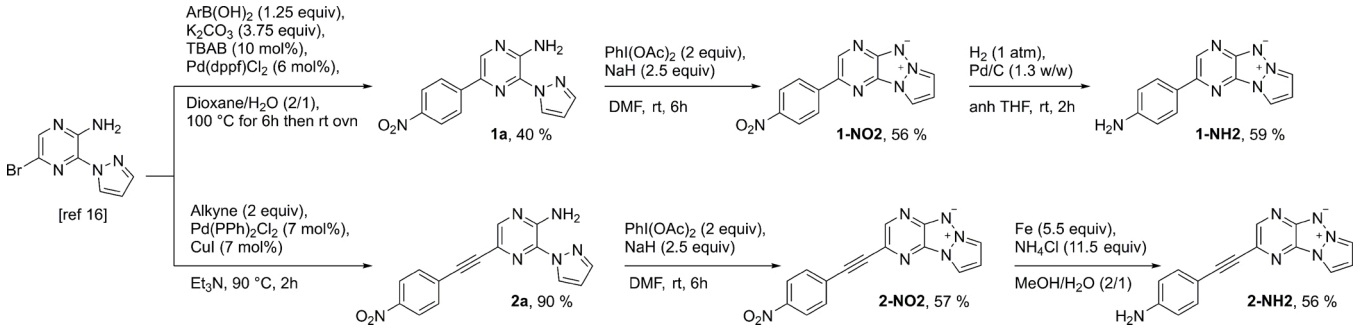

Scheme 1. Preparation of **1-NO$_2$**, **1-NH$_2$**, **2-NO$_2$**, **2-NH$_2$** compounds.

reduction of the nitro moiety proceeding through the nitroso and hydroxylamine intermediates to the fully reduced amino adduct [10]. In type II of NTRs, a reaction can proceed *via* one-electron reduction, resulting in the formation of nitroaromatic anion-free radical intermediates [9], which in the presence of molecular oxygen can be re-oxidized with concomitant formation of superoxide anion radical. This leads to the consumption of reducing equivalents without a net reduction of the nitroaromatic substrate and is called a "futile cycle" [10]. However, in the absence of oxygen or in the presence of a low enough content, the reduction can proceed to the formation of the nitroso intermediate followed by the same steps as for type I NTR. Many of such oxygen-sensitive NTRs were described in mammalian systems [11] and they can be utilized to detect hypoxia *via* the determination of NTR activity.

Over the last decade, many NTRs-sensitive small-molecule probes for NTR determination and for optical imaging of hypoxia were designed and tested in models as well as in living systems [4,12–15]. Most of the NTRs fluorescent probes relied on the attachment of a nitroaromatic moiety to a fluorophore which quenched its fluorescence, while the reduction of nitro moiety catalyzed by NTR resulted in an off-on fluorescence response. Some of the tested probes seemed to be very promising, though, despite many efforts, the transfer of research findings into commercial use, as well as the accessibility of such probes to a wide range of researchers, is very limited. Therefore, a search for better probes for NTR determination is still an open issue. To contribute, we have designed an entirely new type of sensor by conjugating the pyridazino-1,3a,6a-triazapentalene (**PyTAP**, Chart 1) fluorophore (recently discovered by us [16,17]) to a nitrophenyl moiety, which resulted in obtaining compounds that exhibit weak fluorescence (form *off*), which become highly fluorescent (form *on*) upon the reduction by NTR under hypoxic conditions, as shown schematically in Chart 1 . A *para*-nitrophenyl responsive moiety conjugated to PyTAP either directly or with an alkyne linker gave two probes (see Scheme 1) denoted as **1-NO$_2$** and **2-NO$_2$**, as well as their reduced amine counterparts **1-NH$_2$** and **2-NH$_2$**. The response of both probes to NTRs was evaluated with the use of type I oxygen-insensitive NTR from *Escherichia coli* as well as type II oxygen-sensitive NTR using the mammal liver microsomes as its source (see Chart 1). Also, the impact of the interaction between **1-NO$_2$** and **2-NO$_2$** NTR probes and human serum albumin (HSA) was investigated. The *in vitro* evaluation of both probes as hypoxia markers related

to the activity of NTRs was carried out on the highly metastatic human melanoma A2058 cell line.

2. Material and methods

2.1. Synthesis and characterization

2.1.1. General chemistry

Unless otherwise specified, all reagent-grade chemicals and solvents - commercially available, were used without further purification. ^{1}H and ^{13}C NMR spectra were recorded on the Bruker Avance DPX-250 (250 MHz) and Bruker Avance 400 (400 MHz) spectrometers, reporting chemical shifts (δ) in ppm and coupling constants (J) in Hz. Chemical shifts were analyzed in reference to the solvent peaks (DMSO-d_6, $CDCl_3$). High-resolution mass spectra (HRMS) were registered on a Bruker maXis mass spectrometer by the "Fédération de Recherche" ICOA/CBM (FR2708) platform. Low-resolution mass spectra were recorded on a Thermo Scientific Endura mass spectrometer. Thin-layer chromatography (TLC) was performed with the use of aluminum sheets pre-coated Silica Gel 60 F254 (Merck), which were visualized with ultraviolet light at 254 nm. Purification of compounds included the column chromatography on Silica Gel 60 (230−400 mesh, Merck). Melting points were determined using Thermo Scientific 9200 apparatus with capillary tubes. The infrared spectra were recorded on a Thermo Scientific Nicolet iS10 FT-IR and maximum absorption wavenumbers ν" are given in cm^{-1}. Experimental details for the photophysical characterization (absorption and emission spectra, the quantum yield of luminescence (ϕ), the luminescence lifetime (τ) and photostability) are described in Supporting Information.

Additionally, the synthesis of the substrate 1-ethynyl-4-nitrobenzene is presented in the Supporting Information section. Preparation of PyTAP is precisely described in M. Daniel et al. [16].

2.1.2. 5-(4-Nitrophenyl)-3-(1H-pyrazol-1-yl)pyrazin-2-amine (**1a**)

1-Amino-4-bromo-2-pyrazolopyrazine [16] (200 mg, 0.8 mmol), potassium carbonate (460 mg; 3.3 mmol), 4-nitrobenzeneboronic acid (167 mg; 1.0 mmol), TBAB (27 mg; 0.083 mmol), Pd(dppf)Cl_2 (40 mg; 0.05 mmol) were placed in a round-bottom flask and solubilized in a mixture of dioxane/water (0.5 M; 4/1). The reaction was conducted under an argon atmosphere. The mixture was stirred at 100 °C for the first 6 h and then stirring was continued overnight at room temperature. Afterward, the crude mixture was diluted with AcOEt and filtered through Celite. The filtrate was concentrated under reduced pressure. The crude product was purified by column chromatography on silica gel (eluent AcOEt/PE (3/7; 1/1) to obtain the final product **1e -** a red solid (94 mg, 42 %). ^{1}H NMR (250 MHz, DMSO-d_6) δ: 8.91 (d, J =2.6 Hz, 1 H), 8.82 (s, 1 H) 8.37 (d, J =9.0 Hz, 2 H), 8.29 (d, J =9.1 Hz, 2 H), 7.96 (d, J =1.5 Hz, 1 H), 7.91 (s, 2 H), 6.72 (dd, J = 2.7, 1.8 Hz, 1 H). ^{13}C NMR (101 MHz, DMSO-d_6) δ: 146.7, 146.5, 142.3, 141.4, 138.7, 133.7, 131.6, 131.1, 129.3, 128.8, 126.0, 124.1, 107.9. HRMS (ESI) for $C_{13}H_{11}N_6O_2$ $[M+H]^+$ found, 283.0938 *m/z*; calcd mass, 283.0938. Mp: decomposition over 200 °C.

2.1.3. 2-(4-Nitrophenyl)pyrazolo[1',2':1,2][1,2,3]triazolo[4,5-b] pyrazin-6-ium-5-ide (1-NO_2)

In a round-bottom flask, **1e** (198 mg; 0.7 mmol), (diacetoxyiodo) benzene (453 mg; 1.4 mmol;) and sodium hydride (42 mg; 1.7 mmol) were dissolved in degassed DMF. The reaction solution was stirred for 6 h at room temperature. Afterward an extraction of the solution was carried out by adding a mixture of DCM/H_2O. The aqueous phase was washed 3 times with 50 mL of DCM, organic phases were collected, and then the solvent was removed on a rotatory evaporator. The crude compound was purified on silica gel, eluted with a mixture of AcOEt/PE (2/1) and then AcOEt/MeOH (97/3; 92/8), yielding red solid as a product (110 mg, 56 %). ^{1}H NMR (250 MHz, DMSO-d_6) δ: 9.19 (s, 1 H), 8.80 (d, J =3.4 Hz, 1 H), 8.53 (d, J =2.6 Hz, 1 H), 8.40 – 8.29 (m, 4 H), 7.22 (dd, J = 3.4, 2.6 Hz, 1 H). ^{13}C NMR (101 MHz, $CDCl_3$) δ: 149.6, 146.9, 143.6, 141.8, 134.2, 129.8, 126.3, 124.7, 114.1, 112.5, 111.2. HRMS (ESI) for $C_{13}H_9N_6O_2$ $[M+H]^+$ found, 281.0781 *m/z*; calcd mass, 281.0781. Mp: decomposition over 200 °C.

2.1.4. 2-(4-Aminophenyl)pyrazolo[1',2':1,2][1,2,3]triazolo[4,5-b] pyrazin-6-ium-5-ide (1-NH_2)

Under an argon atmosphere, in a round bottom flask, **1-NO_2** (30 mg, 0.1 mmol) was dissolved in anhydrous THF (5 mL). Pd/C (39 mg) was added. Argon was replaced by hydrogen and the reaction mixture was stirred under hydrogen atmosphere for 2 h. The suspension was filtered through Celite and then column chromatography on silica gel was carried out with AcOEt/MeOH (95/5) as an eluent to give the product **1-NH_2** as a red solid (16 mg, 59 %). ^{1}H NMR (400 MHz, DMSO-d_6) δ: 8.86 (s, 1 H), 8.58 (d, J =3.4 Hz, 1 H), 8.33 (d, J =2.6 Hz, 1 H), 7.79 (d, J =8.6 Hz, 2 H), 7.14 (t, J =3.0 Hz, 1 H), 6.67 (d, J =8.9 Hz, 2 H), 5.40 (s, 2 H). ^{13}C NMR (101 MHz, DMSO- d_6) δ: 150.05, 149.16, 138.95, 138.82, 128.08, 126.64, 123.98, 114.02, 110.96, 110.24, 109.25. HRMS (ESI) for $C_{13}H_{11}N_6$ $[M+H]^+$ found, 251.1037 *m/z*; calcd mass, 251.1039. Mp: 192 °C.

2.1.5. 5-((4-Nitrophenyl)ethynyl)-3-(1H-pyrazol-1-yl)pyrazin-2-amine (**2a**)

Under an argon atmosphere, 1-amino-4-bromo-2-pyrazolopyrazine [16] (350 mg, 1.5 mmol), 1-ethynyl-4-nitrobenzene (430 mg, 2.9 mmol) and Pd$(PPh_3)_2Cl_2$ (105 mg, 0.1 mmol) were solubilized in distilled Et_3N (5 mL). The mixture was stirred at room temperature for 20 min and then CuI (25 mg, 0.1 mmol) was added. The solution was stirred at 90 °C for 2 h. The solvent was removed under vacuum and the crude mixture was subjected to column chromatography (EP/AcOEt 7/3 to 0/1) to give **2e** (405 mg, 90 %) as a yellow solid. ^{1}H NMR (250 MHz, DMSO-d_6) δ: 8.65 (d, J =2.6 Hz, 1 H), 8.34 (s, 1 H), 8.31 – 8.23 (m, 2 H), 8.04 (s, 2 H), 7.93 (d, J =1.7 Hz, 1 H), 7.88 – 7.79 (m, 2 H), 6.67 (t, J =2.2 Hz, 1 H). ^{13}C NMR (101 MHz, DMSO-d_6) δ: 146.8, 146.6, 144.8, 141.5, 132.4, 131.6, 129.2, 128.6, 124.0, 121.0, 108.0, 9.74, 87.7. HRMS (ESI) for $C_{15}H_{11}N_6O_2$ $[M+H]^+$ found, 307.0940 *m/z*; clacd mass, 307.0938. Mp: decomposition over 200 °C.

2.1.6. 2-((4-Nitrophenyl)ethynyl)pyrazolo[1',2':1,2][1,2,3]triazolo[4,5-b]pyrazin-6-ium-5-ide (2-NO_2)

2e (126 mg; 0.4 mmol), NaH (25 mg; 1.0 mmol), PhI$(OAc)_2$ (265 mg; 0.8 mmol) were solubilized in degassed DMF (3 mL). The solution was stirred for 6 h at room temperature. DCM/H_2O extraction was carried out and organic phases were collected and concentrated under reduced pressure. Purification involved column chromatography on silica gel with increasing eluent polarity from AcOEt/PE (1/1) to AcOEt to isolate pure **2-NO_2** as a product (106 mg, 57 %). ^{1}H NMR (400 MHz, DMSO-d_6) δ: 8.79 (d, J =3.4 Hz, 1 H), 8.68 (s, 1 H), 8.56 (d, J =2.6 Hz, 1 H), 8.29 (d, J =8.8 Hz, 2 H), 7.85 (d, J =8.8 Hz, 2 H), 7.23 (t, J =3.0 Hz, 1 H) ^{13}C NMR (101 MHz, DMSO-d_6) δ: 146.8, 146.7, 132.3, 128.7, 124.0, 120.5, 114.2, 112.6, 110.8, 92.9, 88.5. HRMS (ESI) for $C_{15}H_9N_6O_2$ $[M+H]^+$ found, 305.0782 *m/z*; clacd mass, 305.0782. Mp: decomposition over 200 °C.

2.1.7. 2-((4-Aminophenyl)ethynyl)pyrazolo[1',2':1,2][1,2,3]triazolo [4,5-b]pyrazin-6-ium-5-ide (2-NH_2)

In a round bottom flask, **2-NO_2** (70 mg, 0.2 mmol) was solubilized in a mixture of MeOH/H_2O (2/1; 7 mL) with the addition of iron powder (64 mg, 1.1 mmol) and NH_4Cl (123 mg, 2.3 mmol). The mixture was stirred mechanically for 36 h. Solvents were removed under vacuum and the crude compound was purified by column chromatography (DCM/MeOH 99/1 to 9/1) to give pure **2-NH_2** (42 mg, 46 %) as a red solid. ^{1}H NMR (400 MHz, DMSO-d_6) δ: 8.70 (d, J =3.4 Hz, 1 H), 8.50 (s, 1 H), 8.46 (d, J =2.6 Hz, 1 H), 7.25 (d, J =8.4 Hz, 2 H), 7.19 (dd, J = 3.4, 2.6 Hz, 1 H), 6.59 (d, J =8.5 Hz, 2 H), 5.65 (s,2 H). ^{13}C NMR (101 MHz, DMSO-d_6) δ: 150.3, 149.8, 145.3, 132.6, 128.6, 123.3, 113.7, 112.9, 111.2, 110.5,

107.4, 92.2, 84.9. HRMS (ESI) for $C_{15}H_{11}N_6$ $[M+H]^+$ found, 275.1642 *m/z*; clacd mass 275.1642. Mp: decomposition over 200 °C.

2.2. General procedure for NTR detection

The reduction of nitro compounds in the presence of NTR was monitored by measuring the emission spectra of the reduced probes from 480 to 700 nm upon excitation at 447 nm. Typical conditions involved 16 μM of **1-NO$_2$** or **2-NO$_2$**, 160 μM NADH, and 2.4 μg/mL NTR from *Escherichia Coli* (Sigma-Aldrich N9284, type I of NTR). The reaction was conducted in 50 mM TRIS-HCl buffer pH 7.4 at 37 °C. Before each measurement, the tested solutions were incubated for 5 min at 37 °C, followed by the addition of the enzyme. A blank solution with **1-NO$_2$** or **2-NO$_2$** and NADH in the absence of NTR was also prepared and measured under the same conditions. To determine the NTR detection limit in the system, fluorescence spectra were measured over time with different NTR concentrations (0–7.2 μg/mL). The fluorescence intensity at 533 nm was plotted against the concentration of NTR and the detection limit was calculated with the following equation: detection limit = 3σ/S where σ is the standard deviation of blank measurements (based on analyzing 11 samples), S is the slope of the fluorescence intensity *vs* NTR concentration denoted as a calibration curve.

2.3. Determination of the reduction products

The overall reduction of nitro compounds in the presence of NTR was monitored by measuring UV–vis spectra. The initial reduction step was too fast to be detected by a conventional spectrophotometer, so it was followed using an Applied Photophysics stopped-flow SX20 Spectrometer. The evolution of the products was registered with a Perkin Elmer HPLC Chromera system equipped with a diode-array detector. A Brownlee Validated IBD C18 5 μm, 150 × 4.6 mm column was employed for the HPLC separation. Separation method: solvent A: 0.1 M ammonium acetate in water, solvent B: CH_3CN; flow rate 1 mL/min; isocratic flow 40 % B from 0 to 6 min; gradient from 40 % to 95 % B at 6 min up to 15 min; isocratic flow 95 % B at 15 min up to 20 min. Chromatograms were recorded using absorbance at 447 nm. To identify the products resulting from the reduction of **1-NO$_2$** or **2-NO$_2$**, LC-HRMS analyses were performed on a Bruker maXis (Q-TOF) mass spectrometer coupled to a Dionex Ultimate 3000 RSLC system. The chromatographic separation was performed at 40 °C on a Phenomenex Kinetex C18 column (150 × 2.1 mm; 1.7 μm) with a flow rate of 0.5 mL/min using a gradient of water + 0.1 % formic acid (solvent A) and acetonitrile + 0.1 % formic acid (solvent B): 3% B from 0 to 0.5 min; 95 % B at 10 min up to 12 min and re-equilibration from 12.1 to 15 min. Mass spectra were recorded in positive mode using an ESI ion source and the formulas were generated using SmartFormula algorithm from DataAnalysis 4.4 software (Bruker) with a mass accuracy of 3 ppm.

2.4. Liver microsomes – source of type II of NTR

Rat liver microsomes (Sigma-Aldrich M9066) were used as a source of type II of NTR. Typical conditions for the reduction involved 16 μM of probes, 1 mM of NADH, and 1 mg/mL of liver microsomes, and the reaction was conducted in 50 mM TRIS-HCl buffer pH 7.4 at 37 °C for 3 or 6 h. The reaction was carried out at air-equilibrated conditions, at hypoxia chamber at 1% pO_2 as well as in a glovebox (Inert, I-Lab) with pO_2 content below 1 ppm. The progress of the reduction and reaction products was determined using HPLC as described above.

2.5. Human serum albumin – interference with NTR detection

The protein stock solution was prepared by dissolving human serum albumin (HSA) in water and its concentration was determined spectrophotometrically from the molar absorptivity of 4.4×10^3 cm^{-1} M^{-1} at 280 nm. The influence of HSA on reduction was characterized using size exclusion chromatography. Typical conditions involved 16 μM of **1-NO$_2$** or **2-NO$_2$**, 160 μM NADH, 2.4 μg/mL NTR as well as 16 μM HSA, and the reaction was conducted in 50 mM TRIS-HCl buffer pH 7.4 at 37 °C. After 1 h of incubation, the reaction mixture was separated by employing BioBasic SEC 300 column. Separation method: solvent: 50 mM Tris-HCl pH 7.4, 150 mM NaCl, 25 mM $NaHCO_3$; flow rate 0.35 mL/min; time of separation 10 min. Chromatograms were recorded using a fluorescence detector with λ_{ext} 490 nm and λ_{em} 550 nm.

2.6. Cell culture conditions

Biological studies were performed using human highly metastatic melanoma A2058 cells line. Cells were cultured in EMEM medium supplemented with 2 mM Glutamine, 1% Non-Essential Amino Acids (NEAA) (v/v), 10 % Fetal Bovine Serum (FBS) (v/v) and 1% penicillin-streptomycin solution (100 units/mL-100 μg/mL) (v/v). Cells were routinely cultured at 37 °C in a humidified incubator in a 5% CO_2 atmosphere. Hypoxic conditions were maintained in a humidified hypoxic chamber (Coy) filled with a gas mixture comprising 94 % N_2, 5% CO_2 and, 1% O_2. For hypoxia screens, cells were seeded under normal conditions and then moved to the hypoxic chamber for at least 24 h pre-incubation. Medium intended to be used in hypoxic experiments was also preincubated in the hypoxic chamber for at least 24 h. Alternatively, cells were incubated with 200 μM of desferrioxamine (DFO) 24 h before further experiments to chemically induce hypoxia. The experimental conditions for the evaluation of cytotoxicity and photocytotoxicity and the uptake of the studied compounds as well as their photostability under *in vitro* conditions were described in Supplementary Information.

2.7. Detection of NTR in cell lysates

Cells were grown under different conditions (hypoxia, normoxia or in the presence of DFO) after 24 h were detached with trypsin, centrifuged, counted, and resuspended in lysis buffer (PBS with 1% Triton-X 100). Lysates were incubated on ice for 30 min and then centrifuged at 13,000 rpm for 20 min at 4 °C. The supernatant was collected, and the protein concentration was determined by Bradford protein assay. Human Nitro reductase (NTR) ELISA Kit (MyBioSource.com) was applied to evaluate the NTR level in cell lysates according to the manufacturer's procedure. Experiments were performed in duplicate to get the mean values ± standard deviation.

2.8. Detection of NTR in cell suspensions

A2058 cells were seeded in a 24-well plate with a density of 3×10^4 cells per cm^2 and kept for 24 h either in normoxia or hypoxic conditions and then incubated with **1-NO$_2$** or **2-NO$_2$** (2 μM) for 2 h. Alternatively, deferoxamine (200 μM) was added and incubated for 6, 18, or 24 h, to cells kept under normoxia for 24 h before this addition and then **1-NO$_2$** or **2-NO$_2$** (2 μM) were added and incubated for 2 h. Next, cells were washed with PBS, detached by trypsin treatment, and analyzed by a BD Versa cytometer (λ_{ext} = 488 nm).

2.9. Bioimaging of cells

A2058 cells were seeded on a 96-well plate with a density of 3×10^4 cells per cm^2 and cultured for 24 h in a medium with FBS under normoxic or hypoxic conditions. Next, (still under hypoxic or normoxic conditions) the **1-NO$_2$** or **2-NO$_2$** (2 μM) were added and incubated for 2 h. Afterward the incubated cells were washed with PBS and fluorescent images were taken using an Olympus IX83 microscope equipped with a CellVivo chamber (λ_{ext} = 470 ± 20 nm, λ_{em} = 525 ± 25).

Table 1
Spectroscopic properties for the triazapentalene compounds in DMSO.

	Absorption		Emission		
	λ_{max}[a] [nm]	ε [M^{-1} cm^{-1}]	λ_{max} [nm]	ϕ[b]	τ[ns]
1-NO_2	466	17900	541	0.0005	–
1-NH_2	468	18200	546	0.76	6.65
2-NO_2	465	14500	541	0.00015	–
2-NH_2	464	17200	542	0.50	6.67
PyTAP	418[c]	15500[c]	516[c]	0.15[c]	–

[a] Maximum of absorption band in visible region of spectrum.
[b] ϕ is the relative fluorescence quantum yield determined using $[Ru(bpy)_3]Cl_2$ (ϕ = 0.028 in H_2O) as a reference standard.
[c] Data taken from reference [17].

3. Results and discussion

3.1. Synthesis and photophysical characterization

We recently synthesized pyridazino-1,3a,6a-triazapentalene derivative (**PyTAP**) [16,17] and reported its excellent fluorescent properties. Considering its condensed and original mesoionic structure, this scaffold was chosen to design a new class of off/on probes for the detection of nitroreductase. For this purpose, we conjugated a nitrophenyl moiety as the sensitive oxido-reductive group to **PyTAP**. The reduced counterparts with a -NH_2 group instead of -NO_2 group were also synthesized to evaluate photophysical properties of the expected reduced probes. The synthetic approach (Scheme 1) was based on the intramolecular metal free N—N bond formation from pyridazinyl amines through the formation of an electrophilic nitrenium species [16]. Starting from bromoaminopyrazine [16], we first introduced the nitrophenyl moieties through a Suzuki cross-coupling reaction with the 4-nitrophenyl boronic acid to obtain **1a** and through a Sonogashira cross-coupling reaction with 4-nitrophenylacethylene to obtain **2a** (Scheme 1). The key N—N bond formation was then conducted in the presence of $PhI(OAc)_2$, NaH in DMF which efficiently formed compounds **1-NO_2** and **2-NO_2** thanks to the favorable electron-withdrawing character of the nitro group in this nitrene mediated cyclization.

The **1-NO_2** and **2-NO_2** probes were designed to act as the "switch off" forms, and the reduced forms **1-NH_2** and **2-NH_2** as the "switch on" forms. Their synthesis involved the reduction of the nitro group by the application of two different reaction conditions. The *para*-nitrophenyl PyTAP derivative (**1-NO_2**) was reduced under hydrogen in the presence of Pd/C to obtain **1-NH_2**, while the *para*-nitrophenyl alkyne derivative (**2-NO_2**) required selective reduction conditions for the NO_2 group in the presence of iron and NH_4Cl to successfully yield **2-NH_2** as the final product.

The photophysical data for all synthesized compounds with the **PyTAP** reference (*i.e.* unsubstituted pyridazino-1,3a,6a-triazapentalene) are collected in Table 1, while their absorption and emission spectra are shown in Fig. A1. For nitro-PyTAP's derivatives, negligible fluorescence was determined due to effective quenching of fluorophore by the nitroaromatic group, which was previously observed for many other compounds [18]. Interestingly, the corresponding amine-derivatives **1-NH_2** and **2-NH_2** exhibited intense fluorescence with a very high quantum yield of 0.76 and 0.50 in DMSO, respectively. The fluorescence of **1-NH_2** and **2-NH_2** in an aqueous solution was very low, with a quantum yield below 0.2 % (Table S1). Such quenching effect of water is well recognized [19] and reported for PyTAP derivatives [17].

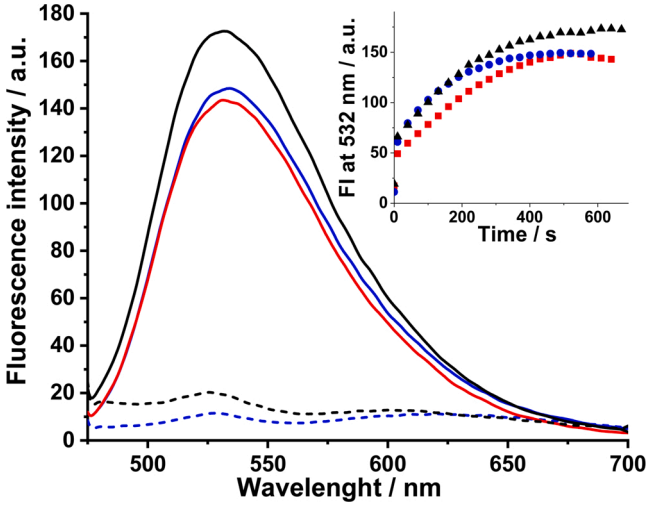

Fig. 2. Fluorescence emission spectra (λ_{ex} = 447 nm) of 16 μM **1-NO_2** (black line) and **2-NO_2** (blue line)) before (dash line), and after (solid line) the reaction with nitroreductase (2.4 μg/mL) taking place in the presence of 160 μM NADH for 15 min in air-equilibrated conditions. The red line denotes the reduction of **2-NO_2** under deoxygenated conditions. Inset: The corresponding time-dependent changes of fluorescence intensity (FI) at 532 nm. TRIS-HCl buffer (pH 7.4, 50 mM), 37 °C. (For interpretation of the references to colour in this figure legend, the reader is referred to the web version of this article).

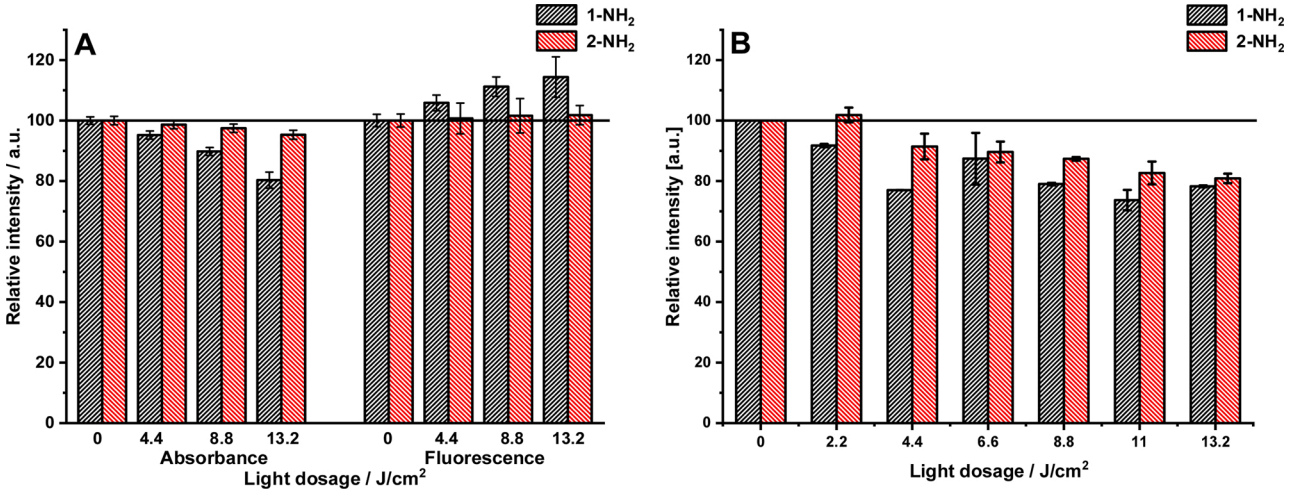

Fig. 1. A) Photostability of **1-NH_2** and **2-NH_2** dissolved in TRIS-HCl buffer (pH 7.4, 50 mM) monitored by registration of changes in absorption (447 nm) and fluorescence (λ_{ex} = 447 nm, λ_{em} = 564 nm) after irradiation at 465 nm. **B**) Photostability *in vitro* of **1-NH_2** and **2-NH_2** tested on A2058 cell line and monitored by registration of changes in fluorescence intensity (λ_{ex} = 447 nm, λ_{em} = 530 nm) after irradiation at 465 nm. The concentration of the compound 40 μM.

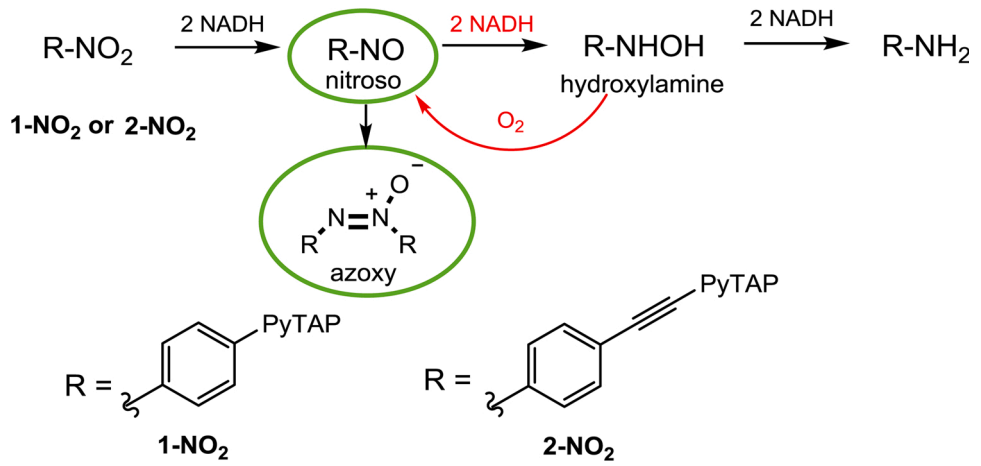

Scheme 2. Major (green circle) and minor products of the **1-NO$_2$** and **2-NO$_2$** probes reduction in the presence of type I nitroreductase under air-equilibrated conditions. (For interpretation of the references to colour in this figure legend, the reader is referred to the web version of this article).

Importantly, the emission of **1-NH$_2$** and **2-NH$_2$** was not quenched by molecular oxygen neither in the aqueous solutions nor in DMSO (Fig. A2), making their fluorescence independent of oxygen. A significant advantage of both probes was, that their amine derivatives were very stable upon irradiation in TRIS buffer, and only a slight decomposition was observed for **1-NH$_2$** (Fig. 1A).

3.2. Probes response to nitroreductase

In these studies, type I oxygen-insensitive NTR from *Escherichia coli* encoded by the *NfsB* gene was used to evaluate the response of **1-NO$_2$** and **2-NO$_2$** probes. Both probes exhibited almost no fluorescence emission upon excitation at 447 nm, however, time-dependent fluorescence enhancement was observed after their co-incubation with NTR and NADH (Fig. 2). As was determined, NADH alone was not able to reduce the tested compounds (Fig. 4). Furthermore, a gradual concentration-dependent decrease in fluorescence intensity caused by dicoumarol (Fig. A3), a competitive inhibitor of NADH [20], proved that the fluorescence off-on response of **1-NO$_2$** and **2-NO$_2$** with regard to NTR was directly related to its enzymatic activity.

The reduction of both probes led to the formation of products with a clear emission maximum at 532 nm and an enhancement of fluorescence intensity by more than 15-fold. As expected, for type I NTR, which catalyzes the reduction of the nitro group by the addition of a pair of electrons independent of the presence of the molecular oxygen [10], the first steps of the reduction in deoxygenated conditions were similar to the observed for the reaction carried out in air-equilibrated conditions (Fig. 2). A relatively fast and gradual increase of the emission intensity was observed within the first 10–15 min (insets in Figs. 2 and A4). Time-dependent absorption spectra showed that the reduction proceeded in several steps (Figs. A5–A7) as was also confirmed by the corresponding chromatograms (Fig. S8). The HRMS analysis of the samples (see Table A2) pointed out that under air-equilibrated conditions the nitroso derivatives of both probes along with azoxy dimers were the predominant products, as is depicted in Scheme A1. The formation of such dimers from nitroso compounds was previously observed for other nitroarenes [21,22]. The studied samples also contained small amounts of the amine counterparts (**1-NH$_2$** and **2-NH$_2$**) as well as traces of the hydroxylamine derivatives, which are unstable under experimental conditions and thus undergo re-oxidation to nitroso derivatives by molecular oxygen. The reduction of nitroso compounds to their hydroxylamine counterparts was continued until the complete depletion of NADH occurred. NADH was introduced to the reactions in 10-fold excess over **1-NO$_2$** or **2-NO$_2$** probes. Since the evolution of the reaction

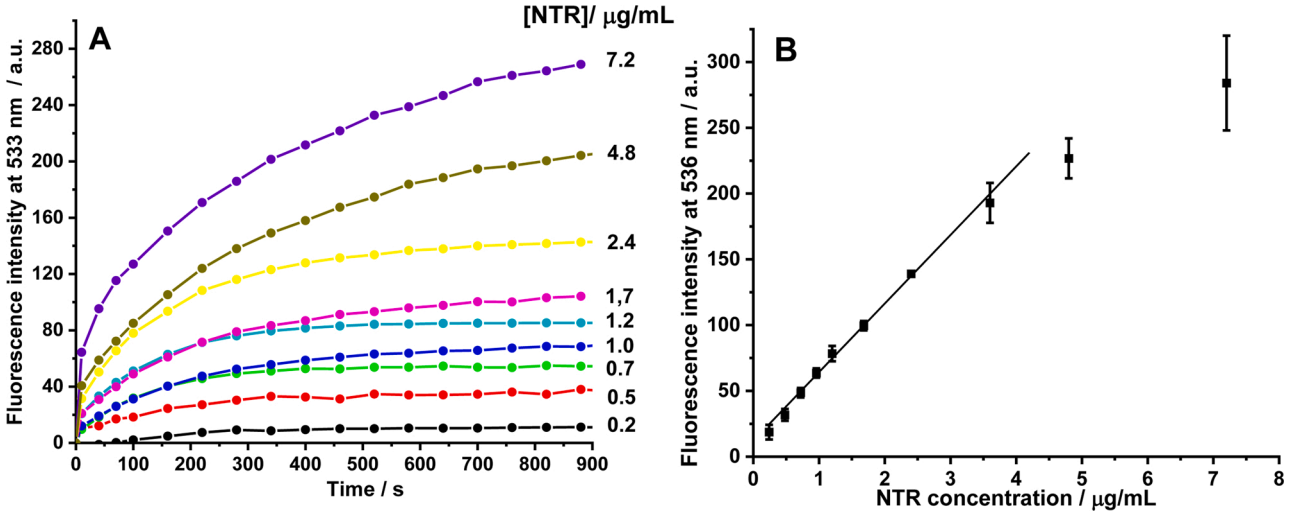

Fig. 3. A) Time-dependent changes of fluorescence intensity (λ_{ex} = 447 nm, λ_{em} = 533 nm) of **2-NO$_2$** (16 µM) in the presence of various concentrations of NTR (0.2 – 7.2 µg/mL) in the presence of 160 µM NADH, TRIS-HCl buffer (pH 7.4, 50 mM), 37 °C; **B**) A correlation between fluorescence intensities and concentrations of NTR after 15 min reaction.

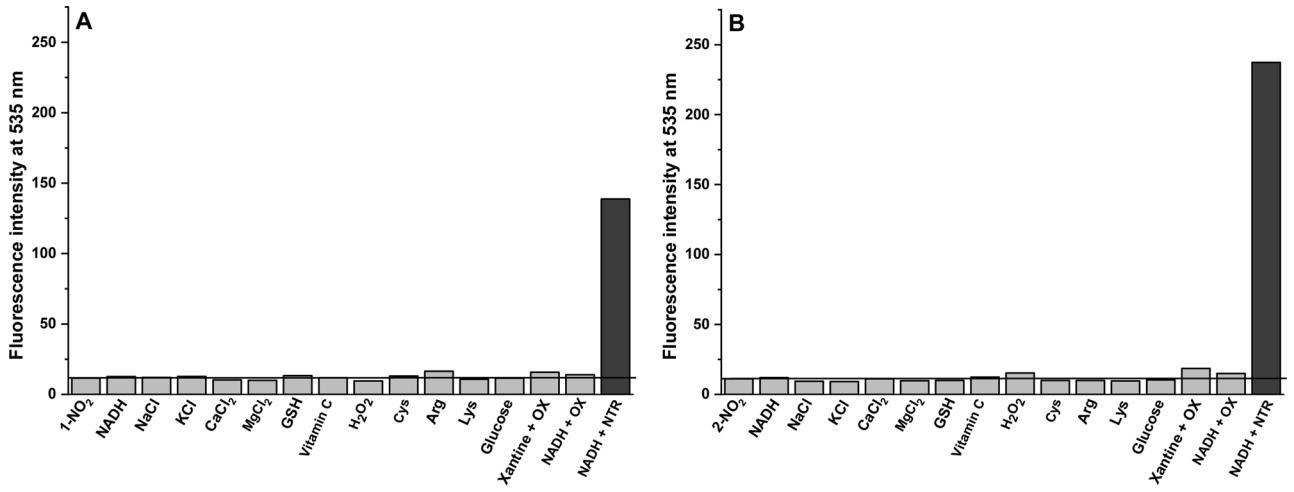

Fig. 4. Fluorescence intensity at 538 nm (λ_{ex} = 447 nm) of 5 μM **1-NO$_2$** (A) and **2-NO$_2$** (B) in solution on its own and in the presence of various reductants: NADH (150 μM), GSH (1 mM), Vitamin C (1 mM), Cys (1 mM); oxidant H_2O_2 (1 mM); salts: NaCl (1 mM), KCl (1 mM), $CaCl_2$ (1 mM), $MgCl_2$ (1 mM), amino acids: Arg (1 mM), Lys (1 mM); glucose (1 mM); xanthine (150 μM) with xanthine oxidase (XO, 0.01U/mL); NADH (150 μM) with xanthine oxidase (0.01U/mL) – grey bars, and NADH (150 μM) with nitroreductase (NTR, 2.4 μg/mL) – black bar. All data were collected 30 min after mixing of reagents and incubation at 37 °C.

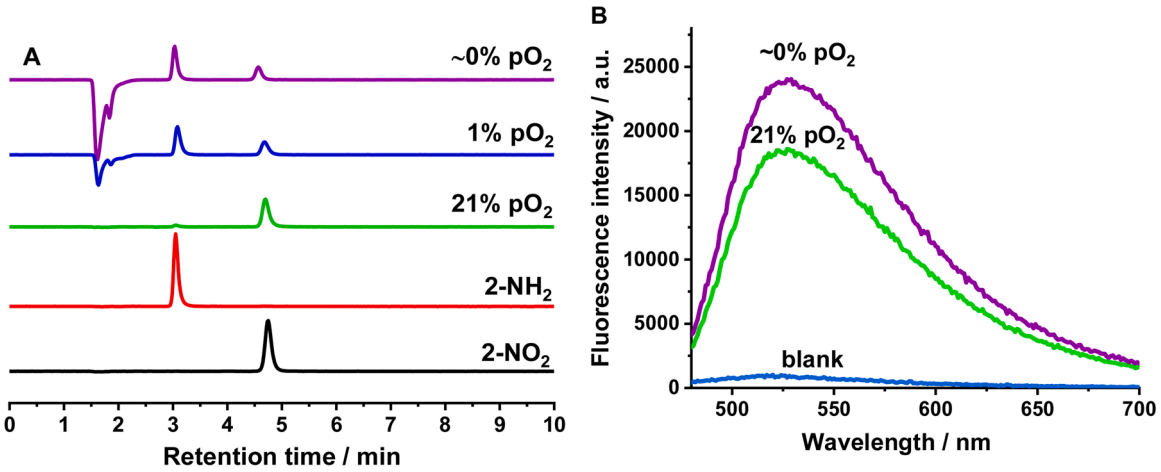

Fig. 5. **A**) Comparison of chromatograms obtained for reduction products of the **2-NO$_2$** probe (16 μM) incubated with NADH (1 mM) and microsomes (1 mg/mL) for 6 h under normoxia (21 % pO_2), hypoxia (1% pO_2), or in the anaerobic environment (< 1 ppm of pO_2, denoted as ~0% pO_2). Chromatograms were recorded using absorbance at 447 nm. B) The emission spectra (λ_{ext} = 466 nm) of microsomes on their own (blank) and after 6 h following the addition of **2-NO$_2$** (16 μM) and NADH (1 mM) kept under normoxic or anaerobic conditions. Experimental conditions: 50 mM TRIS-HCl buffer pH 7.4, 37 °C.

products was oxygen-dependent, when the reaction was carried out under argon, the depletion of NADH was much slower due to a limited excess of oxygen, which resulted in suppressing the re-oxidation reaction (Fig. A7). The reactions taking place in the investigated system were schematically presented in Scheme 2.

The fluorescence of **1-NO$_2$** and **2-NO$_2$** was gradually enhanced with increasing concentration of NTR and a good linear correlation was achieved in the concentration range of 0−4 μg/mL (Figs. 3 and A9). The calculated detection limit was as low as 18.6 and 33.2 ng/mL of NTR for **1-NO$_2$** and **2-NO$_2$**, respectively, according to the 3σ/S standard (σ - standard deviation of blank measurements, S – a slope of calibration curve).

Furthermore, as shown in Fig. 4 the response of the **1-NO$_2$** and **2-NO$_2$** probes to NTR was not affected by different classes of compounds occurring in the intracellular environment, including low molecular weight biological reductants (NADH, GSH, vitamin C, Cys) or oxidants (H_2O_2), inorganic salts (NaCl, KCl, $CaCl_2$, $MgCl_2$), amino acids (Arg, Lys), glucose or other enzymes with the potential to reduce the nitro group (xanthine oxidase) [23]. The obtained data pointed out that the designed compound might be considered a sensitive and selective probe for the determination of NTR.

Liver microsomes were used as a source of mammalian nitroreductases, belonging mainly to the type II of NTRs, which are oxygen-sensitive [9]. The **2-NO$_2$** probe was incubated with microsomes in the presence of NADH for 6 h under different oxygen concentrations. The reduction progress was monitored using HPLC and a plate reader as well (Figs. 5 and A8**C**). The obtained data revealed that the fully reduced product **2-NH$_2$** was only obtained when the reaction was carried out at a very low oxygen concentration (either <1 ppm of pO_2 when kept in a glovebox or 1% pO_2 when kept in a hypoxia chamber) while no reduced product was observed at air-equilibrated conditions (Fig. 5A). The emission from microsomes incubated with **2-NO$_2$** and NADH registered using a plate reader was higher when the reduction was performed under hypoxic conditions (Fig. 5B). The observation of fluorescence under both conditions suggests that the formed nitroso and hydroxylamine intermediates can interact with proteins present in microsomes and this interaction can result in fluorescence enhancement (a similar effect was observed in the presence of HSA as discussed in the next section). Only under oxygen-deprived conditions, the reduction proceeds readily enough to get fully reduced products, which can be

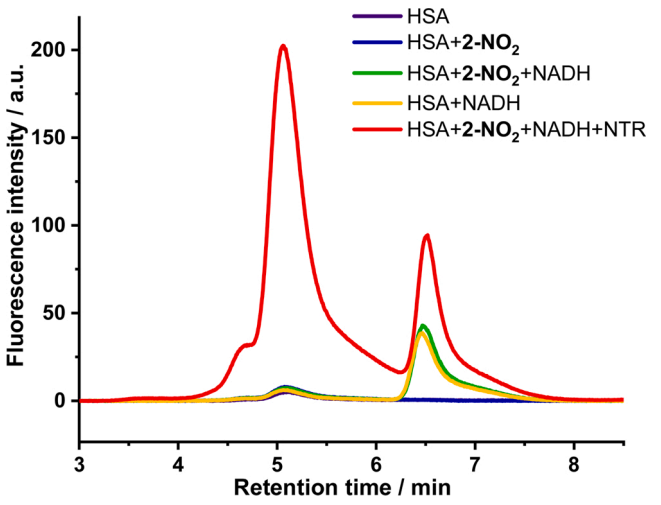

Fig. 6. Size exclusion separation of 16 μM human serum albumin (HSA) incubated in the presence of 16 μM **2-NO$_2$**, 160 μM NADH, 2.4 μg/mL NTR or their mixtures during 1 h. Chromatograms were recorded using a fluorescence detector with λ_{ext} = 490 nm and λ_{em} = 550 nm. Experimental conditions: TRIS-HCl buffer (pH 7.4, 50 mM), 37 °C.

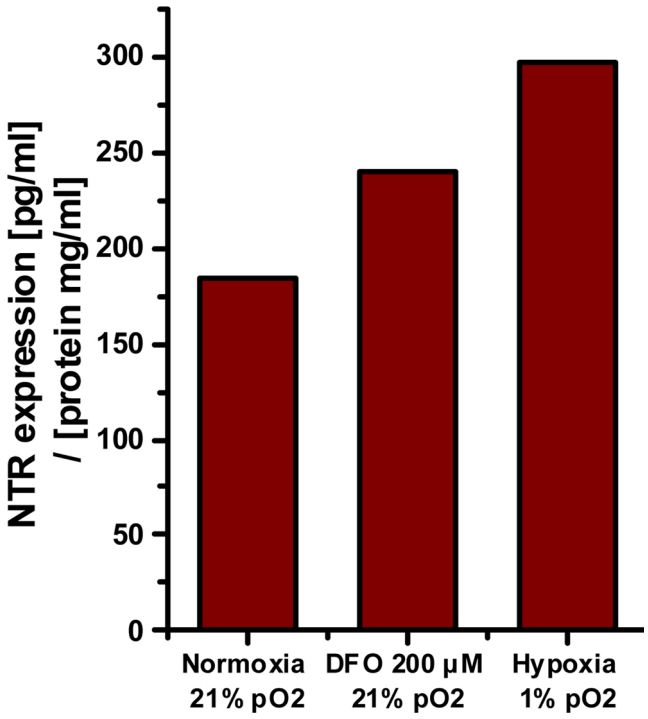

Fig. 7. NTR expression in A2058 cells measured by ELISA after they were exposed to normal (normoxia, 21 % of pO_2) and decreased (hypoxia, 1% of pO_2) oxygen concentration or incubated with 200 μM desferrioxamine (DFO) for 24 h under normoxia.

separated from the protein fraction using HPLC. Collected data strongly supports the relevance of the designed probes in the evaluation of NTR overexpressed in cancer cells (typically type II), the activity of which is strongly related to the presence of oxygen. We believe that fluorescent products generated after the accumulation of probes in hypoxic cells can be further examined in air-equilibrated conditions, typically encountered when using either a plate reader or flow cytometry, since the reduction of these probes will be halted under such conditions. This leads to avoiding the false positive effect and was confirmed by us in *in vitro* studies (vide infra).

3.3. Human serum albumin – interference with NTR detection

The fluorescence of the studied probes and their reduced counterparts was markedly enhanced by the presence of human serum albumin (HSA) in a concentration-dependent manner (see Fig. A10). The increase in emission correlated well with the association constant value for the formation of the studied compound-HSA adducts (see Fig. A11 and Table A3). Presumably, the binding of the studied compounds to HSA results in their protection from external water molecules, thus preventing their quenching [19]. Also, the dielectric constant in the protein environment is much lower than in water [24], which is associated with an increase in the quantum yield of fluorescence. Converting compounds that are not fluorescent in an aqueous solution into highly emissive ones in the presence of HSA was previously reported for other fluorophores [25]. Similar protein-induced fluorescence enhancement (PIFE) effects were observed for carbocyanine dyes linked covalently to DNA, for which the fluorescence intensity greatly increased when a protein was bound in its proximity [26].

HSA can interfere not only with the bioavailability of the probe but also with its response to NTR. Therefore, the activity of NTR was also checked in the presence of HSA by the application of size exclusion chromatography (Figs. 6 and A12). HSA was eluted after 4.82 or 5.06 min as recorded by DAD (280 nm) or fluorescence (λ_{ext} = 490 nm, λ_{em} = 550 nm) detector, respectively. The longer retention time was assigned to low-molecular-weight compounds, in particular to NADH. As clearly shown in Figs. 6 and A12**B** the NTR can reduce both probes in the presence of HSA, however, only in the case of **2-NO$_2$** a pronounced enhancement in the fluorescence was observed. The reduction of the nitro group was slower than in the absence of the protein, which can arise from worsened access of the enzyme to the nitro moiety. Under the experimental conditions, there was a gradual increase in the observed emission even up to 24 h during the incubation with NTR in the presence of HSA, while in the absence of the protein the reaction was over after 0.5 h. The fluorescence signal depends on both the NTR concentration and the time of incubation (Fig. A12**C**). To the best of our knowledge, this report is the first to demonstrate the effect of HSA on the effectiveness of an NTR probe. The results show that binding the probes to the protein does not inactivate them.

3.4. In vitro toxicity and photostability of probes – normoxic and hypoxic conditions

The highly metastatic human melanoma cell line A2058 was selected to assess the *in vitro* properties of both probes. It is known that in melanoma, hypoxia is quite common and is responsible for drug resistance. Moreover, there is a strong correlation between hypoxia and poor patient prognosis, as well as tumor metastasis [27]. In these studies, *in vitro* experiments were carried out on cells, which were grown in normoxic conditions (21 % pO_2), hypoxic conditions using a hypoxic chamber (1% pO_2) as well as in the presence of a chemical, hypoxia-inducing agent desferrioxamine (DFO), which was used to mimic hypoxia in normoxic conditions. DFO, the iron chelator can induce accumulation of the hypoxia-inducible factor-1alpha (HIF-1α) protein, which is a regulator of the cellular response for hypoxia [28,29]. All studied compounds were neither cytotoxic nor photocytotoxic, and the viability of the cells was not disturbed even up to 64 μM concentration of the compounds (Figs. A13–A14). Both amine derivatives were photostable after accumulation in cells, and the degradation was less than 20 % after prolonged irradiation (Fig. 1B). The absence of photobleaching of potential NTR activity products in the cellular microenvironment enables the long-term observation of probes applying an even higher lamp intensity.

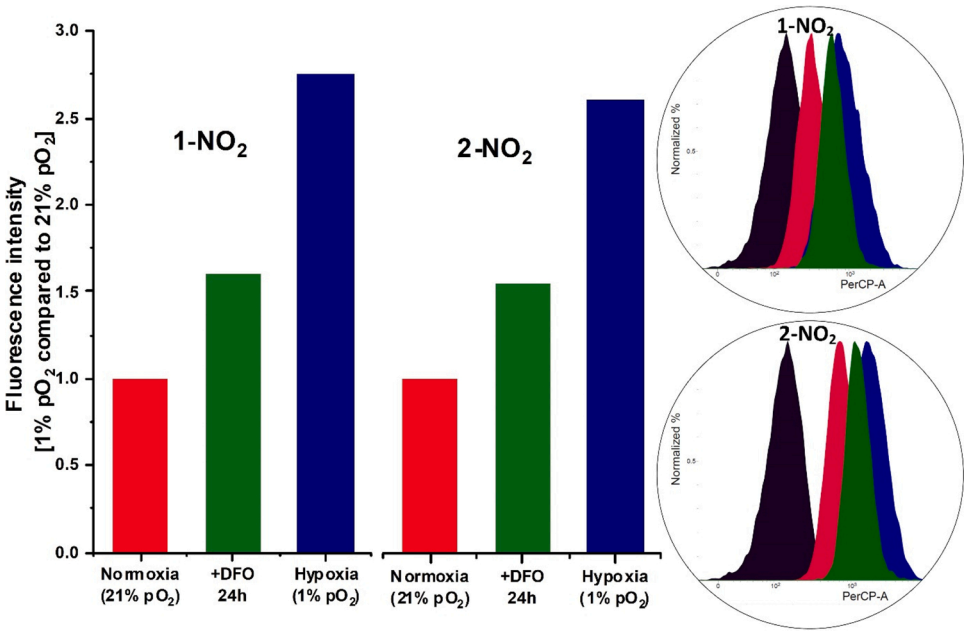

Fig. 8. Relative fluorescence intensity from **1-NO_2** and **2-NO_2** (2 μM) incubated for 2 h with A2058 cells under decreased oxygen concentration (1%) or with cells pre-incubated with 200 μM desferrioxamine (DFO) for 24 h under normoxia (21 %) compared to cells kept under normoxia determined using flow cytometry. In circles: direct data from the cytometer (black – control cells, red – cells under normoxia, green – cells incubated with 200 μM DFO for 24 h, blue – cells under hypoxia). (For interpretation of the references to colour in this figure legend, the reader is referred to the web version of this article).

3.5. *Detection of nitroreductase in cells*

As far as we know, the expression of nitroreductase in A2058 cells has never been assessed. In this study, the amount of NTR was determined in cell lysates using a commercially available human nitroreductase ELISA kit. All cells were lysed after 24 h of growth under normoxic (21 % pO_2) conditions in the absence and presence of 200 μM DFO (desferrioxamine) as well as under hypoxic (1% pO_2) conditions. As

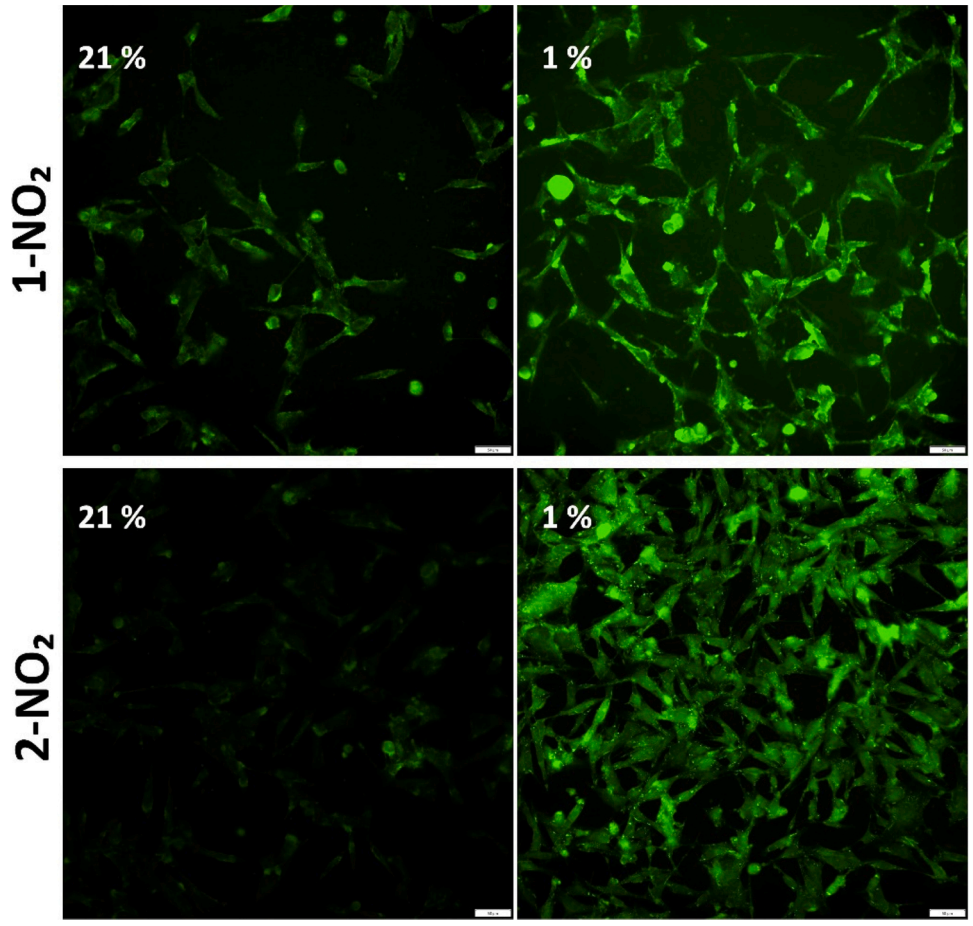

Fig. 9. Fluorescence images of A2058 cells cultured under normoxic (21 % pO_2) and hypoxic (1% pO_2) condition 24 h prior treatment with **1-NO_2** or **2-NO_2** (8 μM) for 2 h.

shown in Fig. 7, A2058 cells produced NTR under normoxia, and its amount increased almost twofold when they were cultured in hypoxic conditions. The amount of NTR was also elevated when hypoxia was chemically induced by DFO, but the increase was smaller. This data confirms that hypoxia can lead to the enhancement of NTR expression in A2058 cells.

The applied ELISA kit involved the lyses of cells, while the **1-NO$_2$** and **2-NO$_2$** probes were designed to identify the changes associated with the hypoxic conditions in the intact cells using either a plate reader or a flow cytometer. Both probes accumulated in A2058 cells quickly and efficiently, and their levels remained unchanged for the first hour (Fig. S15). A pronounced increase in fluorescence intensity of cells was detected after 2 h of incubation, and it can be derived not only from the accumulation of probes, but also their conversion catalyzed by NTR. Therefore, for further experiments, 2 h were chosen as an optimal incubation time. Incubation of cells with **2-NO$_2$** resulted in the detection of a significantly higher fluorescence signal than for **1-NO$_2$**, which can be a result of protein-induced fluorescence enhancement effect observed predominately for **2-NO$_2$** in the presence of albumin.

To test the effectiveness of both sensors *i.e.* **1-NO$_2$** and **2-NO$_2$** in distinguishing between cells cultured under hypoxic and normoxic conditions, probes were incubated with cells for 2 h. Then, cells were washed with PBS buffer, detached using trypsin, resuspended in PBS, and analyzed using a flow cytometer. As shown in Fig. 8 there was a clear difference between cells grown in normoxia compared to those cultured under hypoxia. The fluorescence intensity markedly increased along with the decline of oxygen concentrations and the obtained results pointed out that the reduction of both probes is the reaction responsible for the observed signals. It must be noted that upon excitation at 488 nm the emission from cells can be detected at different channels: FITC (488/527 ± 16 nm), PE (488/586 ± 21 nm), or PerCP (488/700 ± 27 nm) due to sufficient emission even at longer wavelengths (see Fig. A16). This allows minimizing the autofluorescence effect from cells. Furthermore, the application of DFO as a chemical inducer of hypoxic conditions led to lower fluorescence intensity, but it was still clearly distinguishable from cells growth in normoxia. This effect was time-dependent (Fig. A17) and showed that 6 h incubation with DFO was not enough to induce hypoxia in cells. The reduction of probes underwent under all studied conditions, however, it was more pronounced under hypoxic conditions due to the overexpressing of reductase enzymes by cells [7] as a response to hypoxia. As we showed in Fig. 7 NTR was overexpressed under such conditions in A2058 cells, and this enzyme of either Type I or Type II can readily reduce the studied probes. The designed probes allow for a fast assessment of the difference in NTR content for various cell samples without the need for specialized sample preparation.

3.6. Bioimaging applications

A2058 cells incubated with both probes under normoxic conditions showed week fluorescence, while cells treated with the same amount of **1-NO$_2$** or **2-NO$_2$** and cultured under hypoxia prior to the treatment exhibited very bright emission (Fig. 9). It is direct evidence that fluorescence is turned on under hypoxic conditions. This data is a good illustration of the more accurate and sensitive measurements that were made with a flow cytometer (Fig. 8) or a plate reader (Fig. S18). In addition, we expect that the observed difference will be large enough to visually compare two tissues with different NTR activity using a fluorescence microscope. Further *in vivo* studies are needed to evaluate whether the detection of endogenous NTR by both probes can be correlated with the occurrence of hypoxia and whether **1-NO$_2$** and/or **2-NO$_2$** probes can be applied to monitor the hypoxic status of tumor cells.

4. Conclusions

The major outcomes of the investigated probes are schematically presented in Chart 1 . The obtained results clearly showed that the nitropyrazinotriazapentalene derivatives were reduced by both types of NTRs and generated highly fluorescent products. The reaction was sensitive, elective and the formation of products is directly proportional to the amount of the enzyme, with a detection limit as low as *ca.* 20−30 ng/mL of NTR. For oxygen-sensitive NTR present in microsomes, hypoxic conditions allowed a complete reduction of the nitro derivative to its amine counterpart, which was not observed under normoxic conditions. Furthermore, the *in vitro* studies showed that probes readily accumulated in cells without exhibiting host cell toxicity in the concentration range necessary for their application. The obtained data clearly indicates that endogenous NTR is related to hypoxic conditions and the investigated probes were able to evaluate the hypoxia status in tumor cells. It was shown that quantification of hypoxia in cells can be achieved with the use of a plate reader or flow cytometry or can be assessed visually by imaging cells using fluorescence microscopy. The last approach may be helpful in the comparison of tissues collected during a tumor biopsy; however, further *in vivo* studies are needed to support this claim. In the context of *in vivo* tests, it is promising that HSA does not inactivate the reduction of the probes, and the presence of proteins may enhance the fluorescence intensity, which will allow the use of smaller probe concentrations.

CRediT authorship contribution statement

Ewelina Janczy-Cempa and **Olga Mazuryk** investigation, methodology, visualization, and formal analysis for photophysical characterization, NTR and *in vitro* studies. **Olga Mazuryk** validation and supervision for *in vitro* studies. **Doina Sirbu**, **Nicolas Chopin**, **Magdalena Żarnik**, **Magdalena Zastawna** investigation organic synthesis. **Nicolas Chopin** and **Marie-Aude Hiebel** formal analysis, supervision organic synthesis. **Cyril Colas** investigation, formal analysis MS, LC–MS. **Franck Suzenet** and **Małgorzata Brindell** conceptualization, supervision, funding acquisition, writing - original draft, writing - review & editing.

Declaration of Competing Interest

The authors declare that they have no known competing financial interests or personal relationships that could have appeared to influence the work reported in this paper.

Acknowledgements

This work was supported by National Science Center (2019/33/B/NZ7/02980). This work has been supported by la Ligue contre le Cancer (comité du Loiret et des Deux-Sèvres), Labex SynOrg (ANR-11-LABX-0029), Labex IRON (ANR-11-LABX-0018-01), the FEDER TECHSAB, the University of Orleans and the Centre-Val de Loire Region. The project is co-financed by the Polish National Agency for Academic Exchange PHC Polonium.

Appendix A. Supplementary data

Supplementary material related to this article can be found, in the online version, at doi:https://doi.org/10.1016/j.snb.2021.130504.

References

[1] S.-W. LinWu, A.H.-J. Wang, F.-C. Peng, Flavin-containing reductase: new perspective on the detoxification of nitrobenzodiazepine, Expert Opin. Drug Metabol. Toxicol. 6 (2010) 967–981, https://doi.org/10.1517/17425255.2010.482928.

[2] Y. Chen, L. Hu, Design of anticancer prodrugs for reductive activation, Med. Res. Rev. 29 (2009) 29–64, https://doi.org/10.1002/med.20137.

[3] J.N. Copp, A.M. Mowday, E.M. Williams, C.P. Guise, A. Ashoorzadeh, A. V. Sharrock, J.U. Flanagan, J.B. Smaill, A.V. Patterson, D.V. Ackerley, Engineering a multifunctional nitroreductase for improved activation of prodrugs and PET

probes for cancer gene therapy, Cell Chem. Biol. 24 (2017) 391–403, https://doi.org/10.1016/j.chembiol.2017.02.005.
[4] Y.-L. Qi, L. Guo, L.-L. Chen, H. Li, Y.-S. Yang, A.-Q. Jiang, H.-L. Zhu, Recent progress in the design principles, sensing mechanisms, and applications of small-molecule probes for nitroreductases, Coord. Chem. Rev. 421 (2020), 213460, https://doi.org/10.1016/j.ccr.2020.213460.
[5] X. Jing, F. Yang, C. Shao, K. Wei, M. Xie, H. Shen, Y. Shu, Role of hypoxia in cancer therapy by regulating the tumor microenvironment, Mol. Cancer 18 (2019) 157, https://doi.org/10.1186/s12943-019-1089-9.
[6] W.R. Wilson, M.P. Hay, Targeting hypoxia in cancer therapy, Nat. Rev. Cancer 11 (2011) 393–410, https://doi.org/10.1038/nrc3064.
[7] S.A. Fitzsimmons, P. Workman, M. Grever, K. Paull, R. Camalier, A.D. Lewis, Reductase enzyme expression across the national cancer institute tumor cell line panel: correlation with sensitivity to mitomycin C and EO9, J. Natl. Cancer Inst. 88 (1996) 259–269, https://doi.org/10.1093/jnci/88.5.259.
[8] S. Kizaka-Kondoh, H. Konse-Nagasawa, Significance of nitroimidazole compounds and hypoxia-inducible factor-1 for imaging tumor hypoxia, Cancer Sci. 100 (2009) 1366–1373, https://doi.org/10.1111/j.1349-7006.2009.01195.x.
[9] F.J. Peterson, R.P. Mason, J. Hovsepian, J.L. Holtzman, Oxygen-sensitive and -insensitive nitroreduction by Escherichia coli and rat hepatic microsomes, J. Biol. Chem. 254 (1979) 4009–4014, https://doi.org/10.1016/S0021-9258(18)50687-6.
[10] C. Bryant, M. DeLuca, Purification and characterization of an oxygen-insensitive NAD(P)H nitroreductase from enterobacter cloacae, J. Biol. Chem. 266 (1991) 4119–4125, https://doi.org/10.1016/S0021-9258(20)64294-6.
[11] R.P. Mason, J.L. Holtzman, The mechanism of microsomal and mitochondrial nitroreductase. Electron spin resonance evidence for nitroaromatic free radical intermediates, Biochemistry 14 (1975) 1626–1632, https://doi.org/10.1021/bi00679a013.
[12] W. Qin, C. Xu, Y. Zhao, C. Yu, S. Shen, L. Li, W. Huang, Recent progress in small molecule fluorescent probes for nitroreductase, Chin. Chem. Lett. 29 (2018) 1451–1455, https://doi.org/10.1016/j.cclet.2018.04.007.
[13] Z. Zhang, Q. Feng, M. Yang, Y. Tang, A ratiometric fluorescent biosensor based on conjugated polymers for sensitive detection of nitroreductase and hypoxia diagnosis in tumor cells, Sens. Actuatators B Chem. 318 (2020), 128257, https://doi.org/10.1016/j.snb.2020.128257.
[14] L. Xia, F. Hu, J. Huang, N. Lia, Y. Gu, P. Wang, A fluorescent turn-on probe for nitroreductase imaging in living cells and tissues under hypoxia conditions, Sens. Actuatators B Chem. 268 (2018) 70–76, https://doi.org/10.1016/j.snb.2018.04.100.
[15] L.K. Klockow, K.S. Hettie, E.L. LaGory, E.J. Moon, A.J. Giaccia, E.E. Graves, F. T. China, An activatable NIR fluorescent rosol for selectively imaging nitroreductase activity, Sens. Actuatators B Chem. 306 (2020), 127446, https://doi.org/10.1016/j.snb.2019.127446.
[16] M. Daniel, M.-H. Hiebel, G. Guillaumet, E. Pasquinet, F. Suzenet, Intramolecular metal-free N-N bond formation with heteroaromatic amines: mild access to fused-triazapentalene derivatives, Chem. Eur. J. 26 (2020), https://doi.org/10.1002/chem.201905558, 1525-1515-1529.
[17] D. Sirbu, J. Diharce, I. Martinic, N. Chopin, S.V. Eliseeva, G. Guillaumet, S. Petoud, P. Bonnet, F. Suzenet, An original class of small sized molecules as versatile fluorescent probes for cellular imaging, Chem. Commun. 55 (2019) 7776–7779, https://doi.org/10.1039/C9CC03765A.
[18] K. Zhua, T. Qina, C. Zhao, Z. Luo, Y. Huang, B. Liu, L. Wang, A novel fluorescent turn-on probe for highly selective detection of nitroreductase in tumor cells, Sens. Actuatators B Chem. 276 (2018) 397–403, https://doi.org/10.1016/j.snb.2018.08.134.
[19] G.E. Dobretsov, T.I. Syrejschikova, N.V. Smolina, On mechanisms of fluorescence quenching by water, Molecul. Biophys. 59 (2014) 183–188, https://doi.org/10.1134/S0006350914020079.
[20] E. Johansson, G.N. Parkinson, W.A. Denny, S. Neidle, Studies on the nitroreductase prodrug-activating system. Crystal structures of complexes with the inhibitor dicoumarol and dinitrobenzamide prodrugs and of the enzyme active form, J. Med. Chem. 46 (2003) 4009–4020, https://doi.org/10.1021/jm030843b.
[21] B.D. Palmer, P. van Zijl, W.A. Denny, W.R. Wilson, Reductive chemistry of the novel hypoxia-selective cytotoxin 5-[N,N-Bis(2-chloroethyl)amino]-2,4-dinitrobenzamide, J. Med. Chem. 38 (1995) 1229–1241, https://doi.org/10.1021/jm00007a019.
[22] H. Hosoya, L.C. Misal Castro, I. Sultan, Y. Nakajima, T. Ohmura, K. Sato, H. Tsurugi, M. Suginome, K. Mashima, 4,4′-Bipyridyl-catalyzed reduction of nitroarenes by bis(neopentylglycolato)diboron, Org. Lett. 21 (2019) 9812–9817, https://doi.org/10.1021/acs.orglett.9b03419.
[23] K. Tatsumi, A. Inoue, H. Yoshimura, Mode of reactions between xanthine oxidase and aromatic nitro compounds, J. Pharmacobiodyn. (1981) 101–108, https://doi.org/10.1248/bpb1978.4.101.
[24] L. Li, C. Li, Z. Zhang, E. Alexov, On the dielectric “constant” of proteins: smooth dielectric function for macromolecular modeling and its implementation in DelPhi, J. Chem. Theory Comput. 9 (2013) 2126–2136, https://doi.org/10.1021/ct400065j.
[25] G. Dobretsov, B. Polyak, N. Smolina, T. Babushkina, S. Syrejshchikova, T. Klimova, V. Sverbilc, A. Peregudov, Y. Gryzunov, O. Sarkisov, Interaction of a fluorescent probe, CAPIDAN, with human serum albumin, J. Photochem. Photobiol. A Chem. 251 (2013) 134–140, https://doi.org/10.1016/j.jphotochem.2012.11.001.
[26] H. Hwang, S. Myong, Protein induced fluorescence enhancement (PIFE) for probing protein–nucleic acid interactions, Chem. Soc. Rev. 43 (2014) 1221–1229, https://doi.org/10.1039/c3cs60201j.
[27] F.V. Almeida, S.M. Douglass, M.E. Fane, A.T. Weeraratna, Bad company: microenvironmentally mediated resistance to targeted therapy in melanoma, Pigment Cell Melanoma Res. 32 (2019) 237–247, https://doi.org/10.1111/pcmr.12736.
[28] G.L. Semenza, Targeting HIF-1 for cancer therapy, Nat. Rev. Cancer 3 (2003) 721–732, https://doi.org/10.1038/nrc1187.
[29] K.J. Woo, T.-J. Lee, J.-W. Park, T.K. Kwon, Desferrioxamine, an iron chelator, enhances HIF-1a accumulation via cyclooxygenase-2 signaling pathway, Biochem. Biophys. Res. Commun. 343 (2006) 8–14, https://doi.org/10.1016/j.bbrc.2006.02.116.

Ewelina Janczy-Cempa obtained her MSc Degree in Chemistry in 2018 from the Jagiellonian University. She is currently Ph.D. student at the same University. Her scientific interest is mainly devoted to designing sensor for hypoxia assessment.

Olga Mazuryk obtained her Doctoral degree in 2015 from the Jagiellonian University. Currently she is an Assistant Professor of Faculty of Chemistry of the Jagiellonian University. Her research efforts are focused on anticancer effects of metal-based compounds, their bioactivity in hypoxic conditions, and improved delivery.

Doina Sirbu obtained her Doctor Degree in organic chemistry from the University of Orleans in 2016. She is currently working in a pharmaceutical group in Belgium in medical device innovation.

Nicolas Chopin obtained his Doctor Degree in chemistry from Lyon University in 2012. After specialization in fluorescence and therapeutic chemistry, his research interests are drugs and luminescent probes syntheses. He is now working for a chemical company dedicated to the development of various bioactive compounds.

Magdalena Żarnik obtained her MSc Degree in Chemistry in 2018 from the Jagiellonian University and the University of Orléans. She is currently Ph.D. student at the Jagiellonian University and her research focuses on synthesis of small molecular inhibitors targeting protein death 1/protein death ligand one (PD-1/PD-L1) immune checkpoint.

Magdalena Zastawna obtained her MSc Degree in Chemistry in 2016 from the Jagiellonian University and the University of Orléans. Her scientific interests are related to synthesis of new dyes based on the triazapentalene scaffold.

Cyril Colas obtained his Doctor Degree in analytical chemistry from Ecole Polytechnique of Palaiseau in 2006. Now he is a Research Engineer in mass spectrometry at Institute of Organic and Analytical Chemistry at University of Orléans – French National Center for Scientific Research. His current research interests are focused on various aspects of mass spectrometry hyphenated with separation techniques.

Marie-Aude Hiebel obtained her Doctor Degree in organic chemistry from Claude Bernard Lyon 1 University in 2008. Now she is an assistant Professor in Institut de Chimie Organique et Analytique (Orléans University, France) major in organic chemistry. Her current research interests are heterocyclic and medicinal chemistry.

Franck Suzenet obtained his Doctor Degree in chemistry from University of Nantes in 1998. He was appointed at the University of Orleans in 2000 and got a full professor position at the same University in 2014. His research interests are heteroaromatic chemistry for medicinal chemistry and fluorescent probe developments.

Małgorzata Brindell received her Doctoral degree in 2004 from the Jagiellonian University. Since 2018 she has been Professor of the Jagiellonian University and is the Head of the Education Program in Medicinal Chemistry. Her research activities cover many aspects of bioinorganic and medicinal chemistry, among others the application of metal compounds in the treatment and diagnosis of cancer and designing of optical sensors for assessment of hypoxia in tissue.